Research in Microbiology 164 (2013) 164–171

www.elsevier.com/locate/resmic

Effects of intracellular poly(3-hydroxybutyrate) reserves on physiological–biochemical properties and growth of *Ralstonia eutropha*

Tatiana G. Volova [a,b,*], Natalia O. Zhila [a,b], Galina S. Kalacheva [a], Christopher J. Brigham [c], Anthony J. Sinskey [c,d,e]

[a] *Laboratory of Chemoautotrophic Biosynthesis, Institute of Biophysics of the Siberian Branch of The Russian Academy of Sciences, Akademgorodok 50, Krasnoyarsk 660036, Russian Federation*

[b] *Department of Biotechnology, Institute of Fundamental Biology and Biotechnology, Siberian Federal University, 79 Svobodnyi Avenue, Krasnoyarsk 660041, Russian Federation*

[c] *Department of Biology, Massachusetts Institute of Technology, 77 Massachusetts Avenue, Cambridge 02139, MA, USA*

[d] *Health Sciences Technology Division, Massachusetts Institute of Technology, 77 Massachusetts Avenue, Cambridge 02139, MA, USA*

[e] *Engineering Systems Division, Massachusetts Institute of Technology, 77 Massachusetts Avenue, Cambridge 02139, MA, USA*

Received 12 July 2012; accepted 28 September 2012
Available online 23 October 2012

Abstract

Microbial polyhydroxyalkanoates (PHAs), because of their well studied complex physiology and commercial potential, are vehicles for carbon and potential storage reduction for many microbial species. Even with the wealth of studies about microbial PHAs in the scientific literature, polymer accumulation and degradation are still not comprehensively understood. Poly(3-hydroxybutyrate) (P3HB) granule formation and polymer mobility were studied here in the bacterium *Ralstonia eutropha* strain B5786 in autotrophic cultures. Electron microscopy studies revealed decreasing cell size concomitant with enlargement of size and number of intracellular granules, and inhibition of cell division during intracellular polymer production. Activities of key P3HB biosynthetic enzymes demonstrated correlations with each other during polymer accumulation, suggesting an intricately regulated P3HB cycle in autotrophically grown *R. eutropha* cells.

Keywords: Poly(3-hydroxybutyrate); Granules; PHA cycle; *Ralstonia eutropha*

1. Introduction

Polyhydroxyalkanoates (PHAs), microbial carbon and energy storage polyhymers, principally form inclusions (granules) in the bacterial cytoplasm in varying numbers and sizes depending on culture conditions. PHAs are synthesized by many prokaryotes when synthesis of major compounds (protein, nucleic acids, etc.) is reduced, but extracellular carbon is plentiful (Madison and Huisman, 1999). A special role in PHA biosynthesis and granule formation is played by phasins, specific granule-associated proteins that have been extensively studied (Grage et al., 2009; Pötter et al., 2004). Western blot and immunogold labeling reveal the proteinaceous nature of PHA granule surfaces, with the phasin PhaP1 predominating and smaller amounts of PHA synthase (PhaC), PHA-specific regulator protein (PhaR) and PHB depolymerases (PhaZ) (Gerngross et al., 1994; Pötter et al., 2004). There now exist multiple models of PHA granule genesis. The model that was initially proposed is the micelle model (Cho et al., 2012; Ellar et al., 1968; Gerngross et al., 1994; Jendrossek, 2009). There also exists the membrane budding model, suggesting binding of the hydrophobic face of PHA

* Corresponding author. Laboratory of Chemoautotrophic Biosynthesis, Institute of Biophysics of Siberian Branch of The Russian Academy of Sciences, Akademgorodok 50, Krasnoyarsk 660036, Russian Federation. Tel./fax: +7 391 2494428.

E-mail addresses: volova45@mail.ru (T.G. Volova), natasha@ibp.ru (N.O. Zhila), kalach@ibp.ru (G.S. Kalacheva), cbrigham@mit.edu (C.J. Brigham), asinskey@mit.edu (A.J. Sinskey).

0923-2508/$ - see front matter © 2012 Published by Elsevier Masson SAS on behalf of Institut Pasteur.
http://dx.doi.org/10.1016/j.resmic.2012.10.008

synthase to the plasma membrane, from where nascent PHA granules bud, initiating formation of granules with surfaces covered by proteins and a lipid monolayer (Stubbe and Tian, 2003). A third model (Tian et al., 2005b) incorporates the appearance of nascent granules attached to centered, dark-stained, elongated structures known as "mediation elements". The cytoplasmic micelle model was validated using whole-cell electron cryotomography (Beeby et al., 2011). A recent study characterizing epitope-tagged PHA synthase extended the micelle model to include the presence of mediation element enhancements (Cho et al., 2012).

Different strains of *Ralstonia eutropha* (a.k.a. *Cupriavidis necator*) with similar physiological–biochemical and genetic properties dominate the PHA homeostasis research landscape. These strains include *R. eutropha* H16 (ATCC 17699), one of the paradigms of poly(3-hydroxybutyrate) (P3HB) research studied in the US and elsewhere, and strain Z-1 (VKPM B3358), with its fast-growing variant, B5786, investigated in Russia. Strains H16 and B5786 synthesize similar types of PHA polymers (Volova et al., 2007). Comparison of primary amino acid sequences of PHA synthases from these strains showed high homology between the two enzymes (Kozhevnikov et al., 2010). The 16S rRNA gene sequence of strain B5786 (1491 bp, accession number AJ633674) revealed 98.73% similarity to that of H16.

Despite breakthrough studies in the metabolism of hydrogen-oxidizing bacteria, resulting in the construction of an in silico genome-scale model of H16 (Park et al., 2011), thorough understanding of the life cycle of PHA in the *R. eutropha* cell remains elusive. This study thoroughly examines the PHA life cycle by collecting sufficient data from the physiological–biochemical state and growth kinetics of *R. eutropha* cells during granule biogenesis and synthesis through to polymer degradation and utilization.

2. Materials and methods

2.1. Strain and growth conditions

R. eutropha B5786 (Russian National Collection of Industrial Microorganisms, VKPM) was grown autotrophically in 3 L batch cultures in a 10-L laboratory fermentor. The inoculum was prepared by resuspension of a stored culture, maintained on agar plates, into mineral salt medium (Schlegel et al., 1961) with a mixture of CO_2, O_2 and H_2 gases (1:2:6 (v/v)); the cells were batch-cultured in 1 L flasks on an Innova® Incubator Shaker (New Brunswick Scientific, USA) for 25–35 h. The inoculum was then transferred to the fermentor. Initial NH_4Cl concentration in the culture was 1 g/L, and initial cell concentration was not less than 1 g/L (on a dry matter basis). Initial intracellular PHA content did not exceed 10% of the cell dry weight (due to higher polymer content causing an increase in the length of the lag phase of growth). We optimized PHA accumulation using a two-stage batch culture strategy: in the first stage, cells were cultured in a nitrogen-deficient medium (nitrogen supply was approximately 50% of the physiological nitrogen requirement of cells, or 120 mg nitrogen per 1 g of cell biomass synthesized); and in the second stage, the cells were cultivated in nitrogen-free medium (30 °C, pH 7.0) (Volova et al., 1996). When the cell concentration of the cultures reached 2.0–2.5 g/L, an NH_4Cl solution was added to the culture using a peristaltic metering pump at a ratio of approximately 50–60 mg nitrogen per 1 g cell biomass synthesized (NH_4Cl concentration in the culture maintained at 200–300 mg/L). As the cell concentration reached 10 g/L, the nitrogen supply was discontinued and cells were cultivated in nitrogen-free medium (i.e., the second stage) until the cell concentration reached 20–25 g/L.

Intermittently, over the course of the 104 h culture duration, optical densities (via blue light filtered FEK-M colorimeter) and biomass concentrations (washed, then dried for 24 h, at 105 °C) were determined. Gas mixtures were monitored by commercial gas analyzers and an LKhM-80 chromatograph. Fermentation calculations included biomass yield, gas flow rate and yield coefficients on H_2 (Y_{H_2}) g biomass/mol) and O_2 (Y_{O_2}) g biomass/mol).

Cell biomass samples were subjected to the methanolysis procedure (Brandl et al., 1988), and the intracellular polymer concentration was determined by chromatography of fatty acid methyl esters on an Agilent Technologies 7890A gas chromatograph–mass spectrometer (USA). The average rate of PHA synthesis (v) was calculated as follows: $v = dP/dt$, in g/h, where P is the total amount of the polymer synthesized for the time period t. The specific PHA synthesis rate (M, in units of h^{-1}) was calculated for a specific time period over which a certain amount of the polymer was synthesized: $dP/dt = \mu P$, where dP/dt is the polymer synthesis rate, P is the polymer concentration, and μ is the specific synthesis rate (coefficient of proportionality).

2.2. Enzyme assays

Enzymatic assays utilized cell-free extracts. Cells were centrifugally harvested, washed three times and suspended in 0.01 M Tris–HCl buffer, pH 8 (1 g wet biomass/10 mL buffer). Cells were then disrupted by ultrasonic treatment at 4 °C (four pulses × 1 min) and centrifuged at 10,000× g for 10 min.

Specific activities of β-ketothiolase (β-KT), acetoacetyl-CoA reductase (AA-CoA reductase) and hydroxybutyrate dehydrogenase (3HB dehydrogenase) were measured by spectrophotometer (Senior and Dawes, 1973). Poly(3-hydroxybutyrate) (P3HB) synthase activity (Valentin and Steinbüchel, 1994) was measured by a dual-beam recording spectrophotometer (UVICON 943; Kontron Instruments, Milan, Italy). Hydroxybutyrate dehydrogenase assays (oxidative) were performed using dynamics of formation of β-hydroxybutyric acid from calibration graphing of NADH accumulation (340 nm). All activities were calculated in units of μmol/min/mg protein.

All reagents used were sourced from Sigma–Aldrich. Granule-bound PHA depolymerase activity was determined in native polymer granules isolated from *R. eutropha* B5786, using the method developed by Merrick and Doudoroff

(1964). Briefly, cells were resuspended in 0.05 M potassium phosphate buffer, pH 8, ultrasonically disrupted (four pulses × 1 min) and centrifuged in a sucrose gradient (8 mL volume: 2.0, 1.7, 1.3, and 1.0 M solutions) at 100,000× *g* for 3 h (4 °C) on an L5-75 ultracentrifuge (Beckman Instruments, USA). The granule layer between 1.7 and 1.3 M was removed via dialysis against 0.05 M potassium phosphate buffer (pH 8, 10–12 h). Granules were washed with distilled water, centrifuged at 10,000× *g* for 40 min (4 °C) and dispersed in 100 mM Tris–HCl buffer, pH 8.0. To achieve self-hydrolysis, the suspension of granules was diluted with buffer to a final A_{650nm} of 0.5–0.6, producing polymer concentrations of 2–3 g/L. Granule degradation was registered by changes in the absorbance of the granule suspension, which translated to decreasing polymer content (37 °C). To stop the reaction, 10 μl of a 2% Triton X-100 solution was added to the granule suspension. The PHA concentration in granule suspension was determined by a previously described method (Foster et al., 1999). After the reaction was stopped, granules were subjected to methanolysis (Brandl et al., 1988). Methyl esters of fatty acids were analyzed using a gas chromatograph–mass spectrometer (Agilent, USA), as described above. The polymer content was determined using a calibration curve, prepared on the basis of a standard polymer sample which was previously isolated, cleaned and dried to a constant weight. The activity of granule-bound PHA depolymerase is defined as the amount of degraded polymer (mg/min/mg protein).

2.3. Determination of cell and granule size

Cell morphology and P3HB granule formation were studied using scanning electron microscopy (SEM) on a JEM-100C electron microscope. Cells from culture samples were centrifugally harvested at 5000 rpm, washed, and placed on sample stages. Aluminum coating process was performed in a JEE-4C vacuum evaporator (Japan). Cell and granule size and number quantifications used Robotron-BVS image processing with images obtained from a Jenavert reflected light microscope (100X lens, UFK-12 TV camera). Ten fields of 30–50 cells were analyzed per sample.

2.4. Molecular weight analysis

Molecular mass and molecular mass distribution of PHAs were examined using gel permeation chromatography (Agilent Technologies 1260 Infinity, USA) relative to polystyrene reference standards (Sigma, USA). The polymer was recovered from bacterial biomass with dichloromethane. The recovered material was concentrated on a Rotavapor R-210 rotary evaporator (Switzerland) and precipitated in isopropanol. The polymer was dried in a laminar box at 40 °C until the solvent had completely evaporated. A polymer sample (4 mg) was dissolved in chloroform, and a sample of the polymer solution was injected into the chromatograph for molecular weight analysis.

The numbers of average molecular weight (M_n), apparent molecular weight (M_w), and polydispersity (PD) of the PHA were calculated as follows. M_n is the total weight of polymer molecules in a sample divided by the total number of polymer molecules:

$$M_n = \sum (N_i \cdot M_i / N),$$

where N_i is the number of molecules of weight I; N is the total number of molecules; M_i is the weight of molecules of length I.

M_w is a statistical mean value of the relative molecular weight of macromolecules that make up the polymer. M_w was determined from the following equation:

$$M_w = \sum (w_i \cdot M_i),$$

where w_i is mass fraction ($w_i = N_i M_i / \Sigma(N_i \cdot M_i)$.

Polydispersity provides an estimate of proportions of fragments with different degrees of polymerization in the polymer:

$$PD = M_w / M_n.$$

3. Results

3.1. Growth and polymer accumulation in an autotrophic batch culture of R. eutropha B5786

Fig. 1a shows *R. eutropha* B5786 growth and P3HB accumulation from a nitrogen-deficient autotrophic batch culture (samples I–IV represent culture times of 4, 40, 72 and 104 h). As cells of strain B5786, maintained on mineral agar slants at 5 °C, contain a residual <6–9% P3HB (data not shown), culture inoculations were performed using cells containing <10% P3HB. At 4–6 h after inoculation (the beginning of cell growth), cells were beginning to divide and intracellular P3HB concentration was decreasing (Fig. 1a, sample I). In 4–16 h (first phase) cultures, the average and specific P3HB synthesis rates were low, 0.01 g/h and 0.08 h^{-1}, respectively. In subsequent 30–40 h of culture time, both cell and P3HB concentrations increased. At 20–25 h, P3HB content approached 15% of biomass dry weight. During mid-linear growth phase (40 h, sample II), polymer content reached about 50% (Fig. 1a), with average and specific P3HB synthesis rates 0.31 g/h and 0.15 h^{-1}, respectively. After this point, cells were incubated in nitrogen-free medium and P3HB contents increased, with peak content measured during stationary phase (86.0%; Fig. 1a, sample III). Subsequently, P3HB synthesis rates dropped to initial values. Exiting stationary phase and entering polymer utilization, total P3HB gradually decreased, until the intracellular P3HB had finally dropped nearly 4-fold, to 19.3% (Fig. 1a, sample IV).

The highest values of number average (M_n) (509 kDa) and weight average (M_w) (967 kDa) molecular weights were recorded at 40 h of cultivation (i.e., mid-linear growth phase). By the onset of the stationary phase, the molecular weight had decreased, but polydispersity (PD) had increased. During the

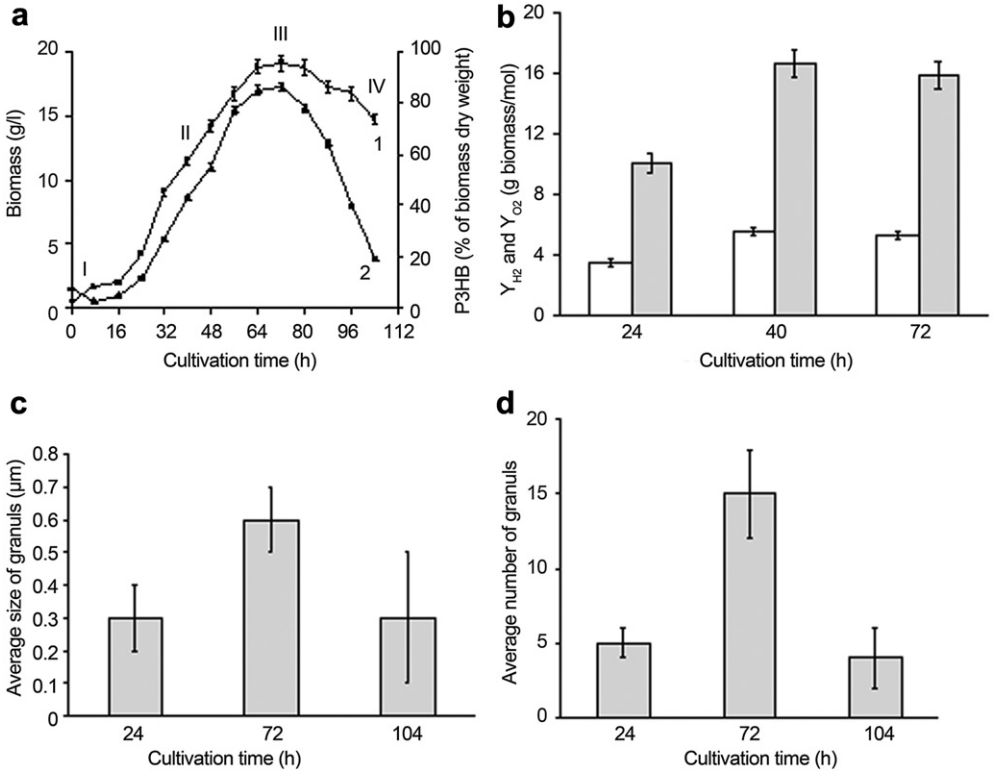

Fig. 1. Biomass (1) and P3HB (2) accumulation in the culture of *R. eutropha* strain B5786 in the stages of growth, PHA accumulation and degradation. Roman numerals indicate sample points in the culture where cell morphology and enzyme activities were observed (a); dynamics of yield coefficients on H_2 (1) and O_2 (2) (g biomass/mol) (b); average size of granules (μm) (c); and average number of granules (d) during cultivation.

polymer degradation phase, the molecular weight decreased and polydispersity increased even more significantly (Table 1).

3.2. Dynamics of gaseous substrate consumption and energy exchange

Previous PHA biosynthesis investigations utilized gaseous CO_2, O_2 and H_2 mixtures despite being weakly soluble and explosive (Ishizaki et al., 2001; Volova et al., 1999). The yield of PHA per unit hydrogen approached 1.0, whereas the yield reached only 0.25–0.3 g/g on alcohols and sugars (Collins, 1987; Lee, 1996). The gas consumption rates change as cultures develop. For *R. eutropha,* initial specific gas consumption rates were H_2: 0.036–0.04 g/(L h), O_2: 0.17–0.18 g/(L h) and CO_2: 0.11–0.14 g/(L h). During the second phase, while accumulating polymer utilizing first-phase metabolites, substrate consumption rates decreased considerably (data not shown).

Table 1
Molecular weights of P3HB synthesized by *R. eutropha* B5786 under autotrophic conditions.

Time (h)	$M_n \times 10^3$ (Da)	$M_w \times 10^3$ (Da)	PD
16	351 ± 15	680 ± 32	1.94 ± 0.07
32	320 ± 12	672 ± 29	2.10 ± 0.12
40	509 ± 12	967 ± 31	1.90 ± 0.11
72	308 ± 11	625 ± 27	2.03 ± 0.09
104	111 ± 8	358 ± 19	3.23 ± 0.16

Average first-phase yield coefficients were H_2: 3.5, O_2: 10.1 g biomass/mol, while in the second phase culture yield coefficients were H_2: 5.6, O_2: 16.7 g biomass/mol (Fig. 1b). Active polymer synthesis accompanied decreasing consumption and oxidation rates of H_2 (energy substrate), demonstrating that non-growing cells consume less energy. During the polymer utilization phase (80–104 h), cell respiratory activity and substrate consumption decreased dramatically, reflecting energy exchange from PHA degradation.

3.3. Dynamics of P3HB cycle enzymes

Table 2 shows specific enzyme activities in *R. eutropha* cell extracts at various time points. After the inoculum was placed in the fermentor, the culture began to grow rapidly and residual intracellular polymer concentration decreased from 8% in the initial inoculum to 1.6% after 8 h of cultivation (a fivefold decrease) (Fig. 1a). During this phase, we recorded peak activities of depolymerizing enzymes (P3HB depolymerase and 3HB dehydrogenase; Table 2). As P3HB synthesis rates increased, the activities of the depolymerizing enzymes decreased. As the first phase ended, activities dropped for β-KT, AA-CoA reductase and P3HB synthase. Upon entering stationary phase, the P3HB content of the cells in culture increased and activities of AA-CoA reductase and P3HB synthase stabilized, but β-KT activity decreased. During P3HB degradation, β-KT activity decreased, P3HB synthase remained level and AA-CoA reductase increased.

Table 2
P3HB biosynthetic and P3HB degradation enzyme activities during growth and polymer production by *R. eutropha* B5786 under autotrophic conditions.

P3HB synthesis enzyme activities (μmol/min mg protein)	Cultivation time (h)			
	8	40	72	104
β-ketothiolase	3.57	1.52	0.80	0.48
acetoacetyl-CoA reductase	0.98	0.61	0.64	1.1
PHA synthase (in soluble cell extract)	0.1	0.005	0.003	0.002
P3HB degradation enzyme activities				
3-hydroxybutyrate dehydrogenase (μmol/min mg protein) (in soluble cell extract)	0.22	0.08	0.01	0.11
PHA depolymerase (mg P3HB/min) (in PHA granules)	0.0021	0.0011	0.0005	0.0007

Activities of the depolymerizing enzymes (P3HB depolymerase and 3HB dehydrogenase) were also examined during P3HB production and utilization (Table 2). Granules extracted at 8 h (with low P3HB content) exhibited the highest depolymerase activities. Granules from the higher polymer content cells (over 50–60% biomass dry weight) showed no autohydrolysis, suggesting low depolymerase activity of cells actively accumulating P3HB. Activity of 3HB dehydrogenase (similar to P3HB depolymerase activity) was highest during the first few hours of the culture. Also, during active P3HB synthesis, dehydrogenase activity decreased and remained at lower levels for 40–50 h before dropping further by the stationary phase. During P3HB degradation (at the end of the experiment, at 104 h), activities of 3HB dehydrogenase and P3HB depolymerase increased compared to the P3HB biosynthesis phase.

We then examined the relationship between the physiological state of polymer-degrading cells and the activity of depolymerizing enzymes of the P3HB cycle. In this case, P3HB degradation was stimulated by depriving the cells of external carbon and energy substrates (CO_2 and H_2). During P3HB degradation under these conditions, depolymerizing enzyme activities changed. Growth substrate supplies to the culture with 45% P3HB were halted after 64 h. Roughly 8 h post-depletion, intracellular polymer concentrations dropped more than 50% and continued to decrease by 0.47 g/h.

At the end of the initial culture growth phase (8 h), the P3HB concentration was only 1.6% and the highest activities of 3HB dehydrogenase and P3HB depolymerase were 0.62–0.80 μmol/min mg protein and 0.066 mg/min, respectively. β-KT and P3HB synthase activities slightly decreased upon nutrient depletion, while AA-CoA reductase activity almost doubled (data not shown). Early in culture, the activities of P3HB metabolism enzymes showed no significant correlations with each other (data not shown). However, clear correlations emerged under substrate deprivation between the rate of P3HB synthesis and the activities of β-KT and P3HB synthase (data not shown).

3.4. Morphology of cells with different P3HB content and P3HB granule formation dynamics

Fig. 2 shows representative SEM images of *R. eutropha* cells. Early growth phase cells (92% contained no polymer; Fig. 2a) were morphologically homogenous (1.0–3.0 μm in length) with the remaining 8% measuring 3–4 μm. During the growth phase, the maximum size was 4 μm. By the mid-linear growth phase (P3HB concentration = 45–50%; Fig. 2b), 59% of cells were still 1–3 μm in length, while the numbers of elongated cells, likely exhibiting impaired cell division, increased and cells of 6 μm in length first appeared. Cell lengths of 3–4 μm constituted 34% of the total. Upon entering stationary phase (86% polymer content; Fig. 2c and d), 64% of the cells exhibited impaired division. Cells ≤4 μm constituted 42% of the observed population, while 20% of cells were of 5–10 μm in length. Some filamentous 20–30-μm-long cells were also observed (Fig. 2c and d).

Entering the polymer utilization phase, with P3HB content decreasing, cell size distributions resembled that of the starting culture. By the end of the experiment (Fig. 2e and f), lengths of 73% cells matched those of typical dividing cells (~1–3 μm length), with 20% 3–4 μm and the remaining 7% ≤ 6 μm.

The images in Fig. 2 demonstrate P3HB granule formation progression during autotrophic culture. The starting culture had no visible polymer granules (Fig. 2a). Early linear growth phase cells contained clearly visible granules (0.2–0.4 μm diameter, 2–8/cell; Fig. 2c and d). In mid-linear growth phase (maximum synthesis rate), average granule size reached 0.5 μm, and most granules were flanked by dark-stained structures. At the highest intracellular polymer concentration, cells were uniformly filled with P3HB granules (≤0.6 μm) whose numbers (some ≥12 granules) depended on the length of the cell (Fig. 2c and d).

Cells in the polymer utilization phase, in contrast to stationary phase cells, had both non-uniform size and varying granule counts (Fig. 2e and f). About 15% of cells contained numerous large (0.5–0.6 μm) granules, but the majority of these cells contained fewer granules with decreased sizes of 0.2–0.3 μm (Fig. 1c and d). Moreover, there were cells observed that contained few or no small granules, indicating that the intracellular polymer was degraded at different rates. The cell size decreased back to 2.5–3.0 μm, and the intracellular protein concentration increased to 49% of the biomass dry weight.

4. Discussion

The idea of "PHA cycle" metabolism was previously discussed in the literature, in a work in which P3HB synthesis was switched to poly(hydroxybutyrate-*co*-hydroxyvalerate) (P(3HB-*co*-3HV) synthesis and simultaneous polymer synthesis and degradation were observed (Doi et al., 1990). Other authors who investigated distribution of radiolabeled polymers during intracellular accumulation and utilization reached a similar conclusion (Taidi et al., 1995). Despite

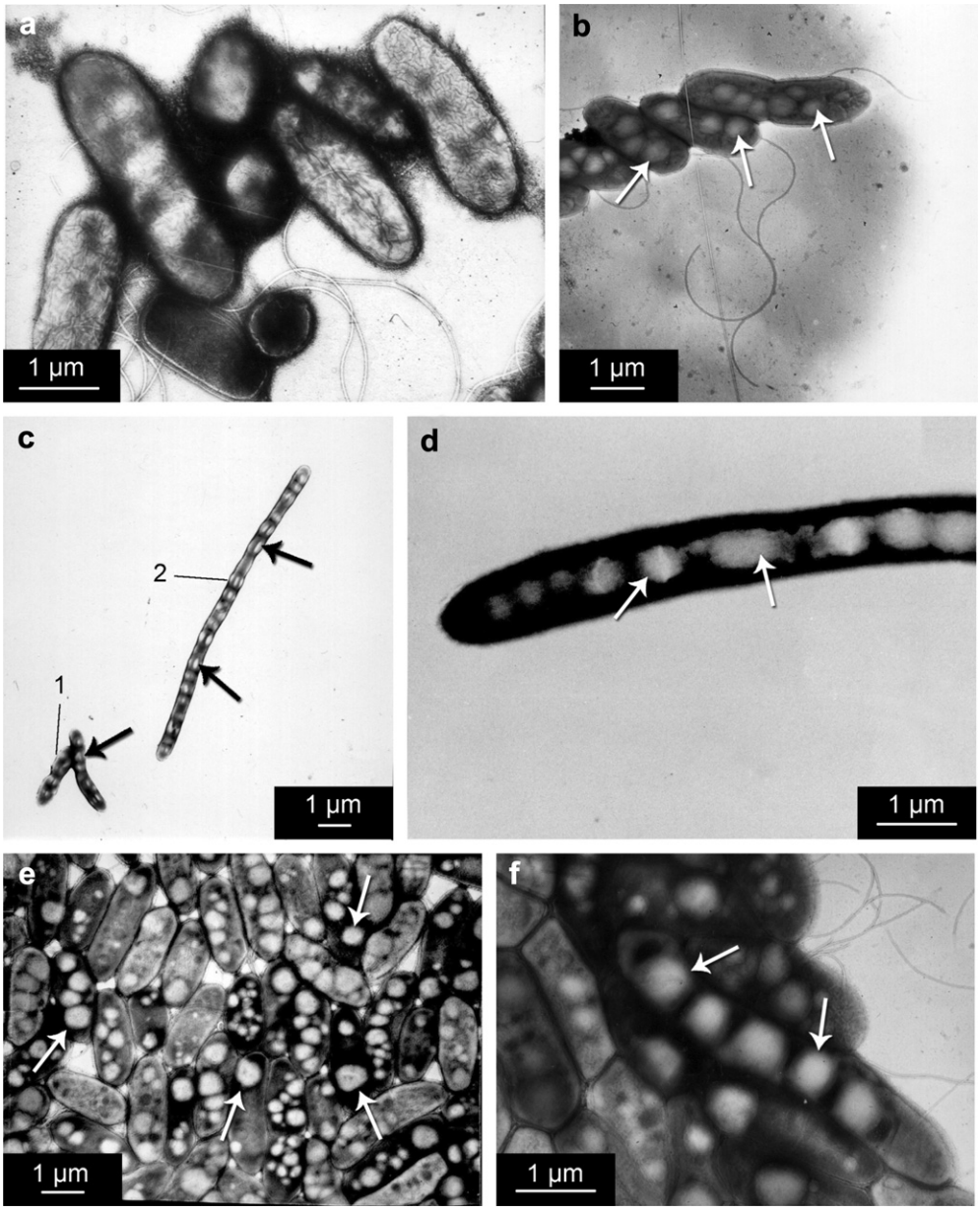

Fig. 2. Representative SEM images of *R. eutropha* B5786 cells from different phases of batch culture during P3HB accumulation under autotrophic conditions. (a) Cells from 4 h of culture, without polymer (sample I); (b) cells from 40 h of culture, containing ~50 wt% P3HB (mid-linear phase, sample II); (c) cells from 72 h of culture, containing 86 wt% (maximum) P3HB (stationary phase, sample III), a giant filamentous *R. eutropha* B5786 cell (1) and a "normal" sized cell (2), also *R. eutropha* B5786); (d) a portion of the giant cell; (e) and (f) cells containing 19.3 wt% P3HB from the polymer degradation phase (104 h) of culture (sample IV). Arrows point to polymer granules.

indirect evidence, few have attempted measurements of intracellular PHA depolymerase activity, given that the substrate is a typically amorphous polymer present in native PHA granules (Saito et al., 1995; Uchino and Saito, 2006; Uchino et al., 2007). Examination of P3HB turnover in radiocarbon-labeled cultures showed that decreasing polymer concentrations matched the decreasing rate of radiolabeled biomass, i.e. turnover was minimal (Haywood et al., 1989). Intracellular polymer degradation rates are potentially an order of magnitude lower than synthesis rates (Doi et al., 1992). In descriptions of PHA granule formation (Ellar et al., 1968; Gerngross et al., 1994), quantitative Western blot analysis demonstrated that PHA synthase and depolymerase enzyme were present simultaneously at key periods in the P3HB cycle (Tian et al., 2005a). While these data confirm the simultaneous presence of synthase and depolymerase, specific regulation of the activities of each enzyme remains unresolved.

The present research presents a comprehensive study of physiological–biochemical properties of *R. eutropha* strain B5786 cultured from early cell growth phases, through PHA accumulation and intracellular PHA degradation using gaseous substrates (H_2, CO_2, and O_2). Although many groups have studied various conditions of PHA synthesis, only one other team (Ishizaki et al., 2001; Tanaka et al., 2011) and the

authors of this study have focused on autotrophic cultivation using gas mixtures.

Key enzyme activities of P3HB metabolism in *R. eutropha* were investigated throughout PHA homeostasis. The highest biosynthetic enzyme activities occurred during increased P3HB synthesis. During accumulation, activities of depolymerizing enzymes (3HB dehydrogenase and PHA depolymerase) were low and exhibited increases in activity only when intracellular polymer degradation was specifically induced by nitrogen addition or carbon removal. Specific activity levels of observed P3HB synthesis enzymes were comparable to *R. eutropha* enzyme activity values from the literature. Previous transcription analysis showed that many genes encoding P3HB production enzymes exhibit similar expression patterns (Lawrence et al., 2005). To our knowledge, this is the only work that provides comprehensive measurements of enzyme activities from batch cultures, ranging from intracellular polymer synthesis to degradation.

Dynamics of PHA granule formation and degradation must be studied in all phases of microbial culture in order to ascertain the relationship of the PHA cycle to the overall physiological activity of the cell. Previously, polymer formation in *R. eutropha* prompted analysis of PHA granule dynamics at different stages of growth and biosynthesis (Tian et al., 2005b), where granule counts and sizes changed with the total amount of intracellular polymer and the age of the culture. Transmission electron microscopy at early P3HB production stages revealed dark-stained structures, (mediation elements) near the center of the cell surrounded by small granules (<0.1 μm diameter). These images promoted a granule formation model in which mediation elements functioned as granule initiation sites. Similar dark-stained structures were seen in cells in the present work, as well as in images of *Comamonas* sp. EB172 cells during early polymer synthesis (Mumtaz et al., 2011). Recent evidence suggests that the nucleoid region of the cell contains these mediation elements and that P3HB granules associate with nucleoid DNA via a newly-discovered granule-associated protein, PhaM (Pfeiffer et al., 2011). In our study, cell sizes were variable in early cell growth and by 72 h growth, small cells dominated. At the highest polymer synthesis rates, we observed an average cell size of 3 μm, with some specimens measuring 10 μm, compared to 2 μm average size during lag phase. We also observed giant cells with a length of 20–30 μm replete with polymer granules, indicating P3HB production in cells with impaired division. Published research shows average volume and total surface area of granules per *R. eutropha* H16 cell at different growth stages (Tian et al., 2005b). Our observations showed that, during peak accumulation, cell granule counts were 10–25. By 72 h, significant granule coalescence occurred and the total surface area of granules was seen to increase. Late-synthesis-phase fusion of granules was also observed in other PHA-accumulating bacteria (Mumtaz et al., 2011; Tay et al., 2010). Moreover, the observation of polymer molecular weight decrease over time agrees with data from other groups (Hori et al., 1994; Shimizu et al., 1993; Taidi et al., 1995).

Entering P3HB utilization, the total polymer content gradually decreased to 19%. However, when cellular metabolism was stimulated by nitrogen-rich media, polymer degradation activity increased and the intracellular polymer concentration dropped to as low as 1.6% (data not shown). The reason why *R. eutropha* cells cannot completely degrade P3HB during utilization is not presently understood. Since the lack of extracellular carbon would constitute a stress condition, the answer may lie in regulation of stress response genes. Cells at the end of the polymer degradation phase were morphologically heterogeneous, with some cells containing granules but others devoid of intracellular polymers. Most cell sizes decreased and the intracellular protein concentration increased. These results clearly show the reversibility of the physiological state of non-dividing, polymer-containing cells and their capacity to become physiologically active again by utilizing intracellular stores of P3HB.

Acknowledgements

This study was financially supported by the project "Biotechnologies of novel biomaterials" (Agreement No. 11.G34.31.0013) in accordance with Resolution No. 220 of the Government of the Russian Federation of April 9, 2010, "On measures designed to attract leading scientists to Russian institutions of higher learning".

References

Beeby, M., Cho, M., Stubbe, J., Jensen, G.J., 2011. Growth and localization of polyhydroxybutyrate granules in *Ralstonia eutropha*. J. Bacteriol. 194, 1092–1099.

Brandl, H., Gross, R.A., Lenz, R.W., Fuller, R.C., 1988. *Pseudomonas oleovorans* as a source of poly(beta-hydroxyalkanoates) for potential applications as biodegradable polyesters. Appl. Environ. Microbiol. 54, 1977–1982.

Cho, M., Brigham, C.J., Sinskey, A.J., Stubbe, J., 2012. Purification of polyhydroxybutyrate synthase from its native organism, *Ralstonia eutropha*: implications for the initiation and elongation of polymer formation *in vivo*. Biochemistry 51, 2276–2288.

Collins, S.H., 1987. Choice of substrates in polyhydroxybutyrate synthesis. Carbon Substr. Biotechnol. 21, 161–169.

Doi, Y., Segawa, A., Kawaguchi, Y., Kunioka, M., 1990. Cyclic nature of poly(3-hydroxyalkanoate) metabolism in *Alcaligenes eutrophus*. FEMS Microbiol. Lett. 67, 165–170.

Doi, Y., Kawaguchi, Y., Koyama, N., Nakamura, S., Hiramitsu, M., Yoshida, Y., Kimura, H., 1992. Synthesis and degradation of polyhydroxyalkanoates in *Alcaligenes eutrophus*. FEMS Microbiol. Lett. 103, 103–108.

Ellar, D., Lundgren, D.G., Okamura, K., Marchessault, R.H., 1968. Morphology of poly-β-hydroxybutyrate granules. J. Mol. Biol. 35, 489–502.

Foster, L.J.R., Lenz, R.W., Fuller, R.C., 1999. Intracellular depolymerase activity in isolated inclusion bodies containing polyhydroxyalkanoates with long alkyl and functional substituents in the side chain. Int. J. Biol. Macromol. 26, 187–192.

Gerngross, T.U., Snell, K.D., Peoples, O.P., Sinskey, A.J., Csuhai, E., Masamune, S., Stubbe, J., 1994. Overexpression and purification of the soluble polyhydroxyalkanoate synthase from *Alcaligenes eutrophus*: evidence for a required posttranslational modification for catalytic activity. Biochemistry 33, 9311–9320.

Grage, K., Jahns, A.C., Parlane, N., Palanisamy, R., Rasiah, I.A., Atwood, J.A., Rehm, B.H.A., 2009. Bacterial polyhydroxyalkanoate granules: biogenesis, structure, and potential use as nano-/micro-beads in biotechnological and biomedical applications. Biomacromolecules 10, 660–669.

Haywood, G.W., Anderson, A.J., Dawes, E.A., 1989. The importance of PHB synthase substrate specificity in polyhydroxyalkanoates synthesis by *Alcaligenes eutrophus*. FEMS Microbiol. Lett. 57, 1–6.

Hori, K., Soga, K., Doi, Y., 1994. Effects of culture conditions on molecular weights of poly(3-hydroxyalkanoates) produced by *Pseudomonas putida* from octanoate. Biotechnol. Lett. 16, 709–714.

Ishizaki, A., Tanaka, K., Taga, N., 2001. Microbial production of poly-D-3-hydroxybutyrate from CO_2. Appl. Microbiol. Biotechnol. 57, 6–12.

Jendrossek, D., 2009. Polyhydroxyalkanoate granules are complex subcellular organelles (carbonosomes). J. Bacteriol. 191, 3195–3202.

Kozhevnikov, I.V., Volova, T.G., Hai, T., Steinbüchel, A., 2010. Cloning and molecular organization of the polyhydroxyalkanoic acid synthase gene of *Ralstonia eutropha* strain B5786. Appl. Biochem. Microbiol. 46, 140–147.

Lawrence, A.G., Schoenheit, J., He, A., Tian, J., Liu, P., Stubbe, J., Sinskey, A.J., 2005. Transcriptional analysis of *Ralstonia eutropha* genes related to poly-(R)-3-hydroxybutyrate homeostasis during batch fermentation. Appl. Microbiol. Biotechnol. 68, 663–672.

Lee, S.Y., 1996. Bacterial polyhydroxyalkanoates. Biotechnol. Bioeng. 49, 1–14.

Madison, L.L., Huisman, G.W., 1999. Metabolic engineering of poly(3-hydroxyalkanoates): from DNA to plastic. Microbiol. Mol. Biol. Rev. 63, 21–53.

Merrick, J.M., Doudoroff, M., 1964. Depolymerization of poly-beta-hydroxybutyrate by intracellular enzyme system. J. Bacteriol. 88, 60–71.

Mumtaz, T., Abd-Aziz, S., Nor'Aini, A.R., Yee, P.L., Wasoh, H., Shirai, Y., Hassan, M.A., 2011. Visualization of core-shell PHBV granules of wild type *Comamonas* sp. EB172 in vivo under transmission electron microscope. Int. J. Polym. Anal. Charact. 16, 228–238.

Park, J.M., Kim, T.Y., Lee, S.Y., 2011. Genome-scale reconstruction and in silico analysis of the *Ralstonia eutropha* H16 for polyhydroxyalkanoate synthesis, lithoautotrophic growth, and 2-methyl citric acid production. BMC Syst. Biol. 5, 101–111.

Pfeiffer, D., Wahl, A., Jendrossek, D., 2011. Identification of a multifunctional protein, PhaM, that determines number, surface to volume ratio, subcellular localization and distribution to daughter cells of poly(3-hydroxybutyrate), PHB, granules in *Ralstonia eutropha* H16. Mol. Microbiol. 82, 936–951.

Pötter, M., Müller, H., Reinecke, F., Wieczorek, R., Fricke, F., Bowien, B., Friedrich, B., Steinbüchel, A., 2004. The complex structure of polyhydroxybutyrate (PHB) granules: four orthologous and paralogous phasins occur in *Ralstonia eutropha*. Microbiology 150, 2301–2311.

Saito, T., Takizava, K., Saegusa, H., 1995. Intracellular poly(3-hydroxybutyrate) depolymerase in *Alcaligenes eutrophus*. Can. J. Microbiol. 41, 187–191.

Schlegel, H.G., Kaltwasser, H., Gottschalk, G., 1961. A submersion method for culture of hydrogen-oxidizing bacteria: growth physiological studies. Arch. Microbiol. 38, 209–222.

Senior, P.J., Dawes, E.A., 1973. The regulation of poly-beta-hydroxybutyrate metabolism in *Azotobacter beijerinckii*. Biochem. J. 134, 225–238.

Shimizu, H., Tamura, S., Shioya, S., Suga, K.-I., 1993. Kinetic study of poly-D(-)-3-hydroxybutyric acid (PHB) production and its molecular weight distribution control in a fed-batch culture of *Alcaligenes eutrophus*. J. Ferment. Bioeng. 76, 465–469.

Stubbe, J., Tian, J., 2003. Polyhydroxyalkanoate (PHA) hemeostasis: the role of PHA synthase. Nat. Prod. Rep. 20, 445–457.

Taidi, B., Mansfield, D.A., Anderson, A.J., 1995. Turnover of poly(3-hydroxybutyrate) (PHB) and its influence on the molecular mass of the polymer accumulated by *Alcaligenes eutrophus* during batch culture. FEMS Microbiol. Lett. 129, 201–205.

Tanaka, K., Miyawaki, K., Yamaguchi, A., Khosravi-Darani, K., Matsusaki, H., 2011. Cell growth and P(3HB) accumulation from CO_2 of a carbon monoxide-tolerant hydrogen-oxidizing bacterium, *Ideonella* sp. O-1. Appl. Microbiol. Biotechnol. 92, 1161–1169.

Tay, B.Y., Lokesh, B.E., Lee, C.Y., Sudesh, K., 2010. Polyhydroxyalkanoate (PHA) accumulating bacteria from the gut of higher termite *Macrotermes carbonarius* (Blattodea: Termitidae). World J. Microbiol. Biotechnol. 26, 1015–1024.

Tian, J., He, A., Lawrence, A.G., Liu, P., Watson, N., Sinskey, A.J., Stubbe, J., 2005a. Analysis of transient polyhydroxybutyrate production in *Wautersia eutropha* H16 by quantitative Western analysis and transmission electron microscopy. J. Bacteriol. 187, 3825–3832.

Tian, J., Sinskey, A.J., Stubbe, J., 2005b. Kinetic studies of polyhydroxybutyrate granule formation in *Wautersia eutropha* H16 by transmission electron microscopy. J. Bacteriol. 187, 3814–3824.

Uchino, K., Saito, T., 2006. Thiolysis of poly(3-hydroxybutyrate) with polyhydroxyalkanoate synthase from *Ralstonia eutropha*. J. Biochem. 139, 615–621.

Uchino, K., Saito, T., Gebauer, B., Jendrossek, D., 2007. Isolated poly(3-hydroxybutyrate) (PHB) granules are complex bacterial organelles catalyzing formation of PHB from acetyl coenzyme A (CoA) and degradation of PHB to acetyl-CoA. J. Bacteriol. 189, 8250–8256.

Valentin, H.E., Steinbüchel, A., 1994. Application of enzymatically synthesized short-chain-length hydroxy fatty acid coenzyme A thioesters for assay of polyhydroxyalkanoic acid biosynthesis. Appl. Microbiol. Biotechnol. 40, 699–709.

Volova, T.G., Kalacheva, G.S., Konstantinova, V.M., 1996. A technique of producing a heteropolymer of β-hydroxybutyric and β-hydroxyvaleric acids. Patent N 2051968 (Russian Federation).

Volova, T., Gitelson, J., Terskov, I., Sidko, F., 1999. Hydrogen bacteria as a potential regenerative LSS component and producer of ecologically clean degradable plastic. Life Support. Biosph. Sci. 6, 209–213.

Volova, T.G., Kalacheva, G.S., Kozhevnikov, I.V., Steinbüchel, A., 2007. Biosynthesis of multicomponent polyhydroxyalkanoates by *Wautersia eutropha*. Microbiology 76, 704–711.